Stochastic Turing patterns in the Brusselator model

Tommaso Biancalani
Dipartimento di Fisica, Università degli Studi di Firenze, via G. Sansone 1, 50019 Sesto Fiorentino, Florence, Italy

Duccio Fanelli
Dipartimento di Energetica, Università degli Studi di Firenze, via S. Marta 3, 50139 Florence, Italy and INFN, Sezione di Firenze, via G. Sansone 1, 50019 Sesto Fiorentino, Florence, Italy

Francesca Di Patti
Dipartimento di Fisica "Galileo Galilei," Università degli Studi di Padova, via F. Marzolo 8, 35131 Padova, Italy
(Received 26 October 2009; revised manuscript received 4 February 2010; published 27 April 2010)

A stochastic version of the Brusselator model is proposed and studied via the system size expansion. The mean-field equations are derived and shown to yield to organized Turing patterns within a specific parameters region. When determining the Turing condition for instability, we pay particular attention to the role of cross-diffusive terms, often neglected in the heuristic derivation of reaction-diffusion schemes. Stochastic fluctuations are shown to give rise to spatially ordered solutions, sharing the same quantitative characteristic of the mean-field based Turing scenario, in term of excited wavelengths. Interestingly, the region of parameter yielding to the stochastic self-organization is wider than that determined via the conventional Turing approach, suggesting that the condition for spatial order to appear can be less stringent than customarily believed.

DOI: 10.1103/PhysRevE.81.046215 PACS number(s): 89.75.Kd, 87.23.Cc, 87.10.Mn, 02.50.Ey

I. INTRODUCTION

Turing instability constitutes a universal paradigm for the spontaneous generation of spatially organized patterns [1]. It formally applies to a wide category of phenomena, which can be modeled via the so called reaction-diffusion schemes. These are mathematical models that describe the coupled evolution of spatially distributed species, as driven by microscopic reactions and freely diffusing in the embedding medium. Diffusion can potentially seed the instability by perturbing the mean-field homogeneous state, through an activator-inhibitor mechanism, and so yielding to the emergence of patched, spatially inhomogeneous, density distribution [2]. The realm of application of the Turing ideas encompasses different fields, ranging from chemistry to biology, from ecology to physics. The most astonishing examples, as already evidenced in Turing original paper, are perhaps encountered in the context of morphogenesis, the branch of embryology devoted to investigating the development of patterns and forms in biology [3].

Beyond the qualitative agreement, one difficulty in establishing a quantitative link between theory and empirical observations has to do with the strict conditions for which the organized Turing patterns are predicted to occur. In particular, and with reference to simple predator-prey competing populations, the relative degree of diffusivity of the interacting species has to be large according to the theory prescriptions, and at variance with the direct experimental evidence. Moreover, patterns formation appears to be rather robust in nature, as opposed to the Turing predictive scenario, where a fine tuning of the parameters is often necessary.

In [4] it was demonstrated that collective temporal oscillations can spontaneously emerge in a model of population dynamics, as due to a resonance mechanism that amplifies the unavoidable intrinsic noise, originating from the discreteness of the system. Later on an extension of the model was proposed [5] so to explicitly account for the notion of space. It was in particularly shown that the number density of the interacting species oscillates both in time and space, a macroscopic effect resulting from the amplification of the stochastic fluctuations about the time independent solution of the deterministic equations. More recently, Butler and Goldenfeld [6] proved that persistent spatial patterns and temporal oscillations induced by demographic noise, can develop in a simple predator-prey model of plankton-herbivore dynamics. The model considered by the authors of [6] exhibits a Turing order in the mean field theory. The effect of intrinsic noise translates however into an enlargement of the parameter region yielding to the Turing mechanism, when compared to its homologous domain predicted within the conventional linear stability analysis. This is an individual based effect, which has to be accommodated for in any sensible model of natural phenomena, and which lacks in the Turing interpretative scenario, that formally applies to the idealized continuum limit. Interestingly, as reported in [7], the discreteness of the scrutinized medium can yield to robust spatio-temporal structures, also when the system does not undergo Turing order in its mean-field, deterministic version.

Starting from this setting, we present the results of our investigations carried out for a spatial version of the Brusselator model, which we shall be introducing in the forthcoming section. As opposed to the analysis in [6], we will operate within the so called urn protocol, where individual elements belonging to the inspected species are assumed to populate an assigned container. The proposed formulation of the Brusselator differs from the one customarily reported in the literature. Additional terms are in fact obtained building on the underlying microscopic picture. These latter contributions are generally omitted, an assumption that we interpret as working in a diluted limit. Interestingly, the phase diagram of the homogeneous (aspatial) version of the model, is remark-

ably different from its diluted analogue, a fact we will substantiate in the following.

Furthermore, when constructing the mean-field dynamics from the assigned microscopic rules, one recovers nontrivial cross-diffusive terms, as previously remarked in [5]. These are derived within a self-consistent analysis and ultimately stands from assuming a finite carrying capacity in a given spatial patch. As such, they potentially bear an important physical meaning, which deserves to be further elucidated. This scheme, alternative to conventional reaction-diffusion models, calls for an extension of the original Turing condition, that we will derive in the following. This is the second result of the paper.

Finally, by making use of the van Kampen system size expansion, we are able to estimate the power spectrum of fluctuations analytically and so delineate the boundaries of the spatially ordered domain in the relevant parameters' space. As already remarked in [6], the role played by the intimate graininess can impact dramatically the Turing vision, returning a generalized scenario that holds promise to bridge the gap with observations.

II. SPATIAL VERSION OF THE BRUSSELATOR MODEL

The Brusselator model represents a paradigmatic example of an autocatalytic chemical reaction. This scheme was originally devised in 1971 by Prigogine and Glandsdorff [8] and quickly gained its reputation as the prototype model for oscillating chemical reaction of the Belosouv-Zhabotinsky [9,10] type. In the following we shall consider a slightly modified version of the original formulation, where the number of reactants X and Y is conserved and totals in N, including the empties, here called E [4]. Moreover we will consider a spatially extended system composed of Ω cells, each of size l, where reactions are supposed to occur [13]. Practically each cell hosts a replica of the Brusselator system: the molecules are however allowed to migrate between adjacent cells, which in turn implies an effective spatial coupling imputed to the microscopic molecular diffusion. A periodic geometry is also assumed so to restore the translational invariance. Although the calculation can be carried out in *any* space dimension D (see [5,7]) we shall here mainly refer to the $D=1$ case study, so to privilege the clarity of the message over technical complications. It should be however remarked that our conclusions are general and remain unchanged in extended spatial settings. Mathematically, the model can be cast in the form

$$A + E_i \xrightarrow{a} A + X_i,$$

$$X_i + B \xrightarrow{b} Y_i + B,$$

$$2X_i + Y_i \xrightarrow{c} 3X_i,$$

$$X_i \xrightarrow{d} E_i,$$

where the index i runs from 1 to Ω and identifies the cell where the molecules are located. The autocatalytic species of interest to us are X_i and Y_i. The elements A and B work as enzymatic activators, and keep constant in number. As such, they can be straightforwardly absorbed into the definition of the reaction rates. Let us label with n_i (respectively, m_i and o_i) the number of element of type X_i (respectively, Y_i and E_i) populating cell i. Then, assuming N to identify the maximum number of available cases within each cell, one gets $N=n_i+m_i+o_i$ a condition, which can be exploited to reduce the actual number of dynamical variables to two. The dynamics of the model is ultimately related to studying the coupled interaction between the discrete species n_i and m_i. The migration between neighbors cells is specified through

$$X_i + E_j \xrightarrow{\mu} E_i + X_j,$$

$$Y_i + E_j \xrightarrow{\delta} E_i + Y_j.$$

Assuming a perfect mixing in each individual cell i, the transition probabilities $T(\cdot|\cdot)$ read [4]

$$T(n_i+1,m_i|n_i,m_i) = a\frac{N-n_i-m_i}{N\Omega},$$

$$T(n_i-1,m_i+1|n_i,m_i) = b\frac{n_i}{N\Omega},$$

$$T(n_i+1,m_i-1|n_i,m_i) = d\frac{n_i^2 m_i}{N^3\Omega},$$

$$T(n_i-1,m_i|n_i,m_i) = c\frac{n_i}{N\Omega}, \tag{1}$$

where according to the standard convention, the rightmost input specifies the original state and the other entry stems for the final one. In addition, the migration mechanism between neighbors cell is controlled by

$$T(n_i-1,n_j+1|n_i,n_j) = \mu\frac{n_i}{N}\frac{N-n_j-m_j}{N\Omega z},$$

$$T(m_i-1,m_j+1|m_i,m_j) = \delta\frac{m_i}{N}\frac{N-n_j-m_j}{N\Omega z}, \tag{2}$$

where the positive constants μ and δ quantify the diffusion ability of the two species and z stands for the number of first neighbors. To complete the notation setting, we introduce the Ω-dimensional vectors $\mathbf{n}$ and $\mathbf{m}$ to identify the state of the system. Their i-th components, respectively, read n_i and m_i.

The aforementioned system is intrinsically stochastic. At time t there exists a finite probability to observe the system in the state characterized by $\mathbf{n}$ and $\mathbf{m}$. Let us label $P(\mathbf{n},\mathbf{m},t)$ such a probability. One can then write down the so-called master equation, a differential equation, which governs the dynamical evolution of the quantity $P(\mathbf{n},\mathbf{m},t)$. The master equation for the case at hand takes the form

$$\frac{\partial}{\partial t}P(\mathbf{n},\mathbf{m},t) = \sum_{i}^{\Omega}[(\epsilon_{X_i}^{-}-1)T(n_i+1,m_i|n_i,m_i) + (\epsilon_{X_i}^{+}-1)T(n_i-1,m_i,|n_i,m_i) + (\epsilon_{X_i}^{+}\epsilon_{Y,i}^{-}-1)T(n_i-1,m_i+1|n_i,m_i) + (\epsilon_{X_i}^{-}\epsilon_{Y_i}^{+}-1)T(n_i+1,m_i-1|n_i,m_i) + \sum_{j\in i}[(\epsilon_{X_i}^{+}\epsilon_{X_j}^{-}-1)T(n_i-1,n_j+1|n_i,n_j) + (\epsilon_{Y_i}^{+}\epsilon_{Y_j}^{-}-1)T(m_i-1,m_j+1|m_i,m_j)]] \times P(\mathbf{n},\mathbf{m},t), \quad (3)$$

where use has been made of the definition of the step operators

$$\epsilon_{X_i}^{\pm}f(\ldots,n_i,\ldots,\mathbf{m}) = f(\ldots,n_i\pm 1,\ldots,\mathbf{m}),$$

$$\epsilon_{Y_i}^{\pm}f(\mathbf{n},\ldots,m_i,\ldots) = f(\mathbf{n},\ldots,m_i\pm 1,\ldots), \quad (4)$$

and where the second sum in Eq. (3) runs on first neighbors $j\in i$. Equation (3) is exact, the underlying dynamics being a Markov process. The master equation (3) contains information on both the ideal mean-field dynamics (formally recovered in the limit of diverging system size) and the finite N corrections. To bring into evidence those two components, one can proceed according to the prescriptions of van Kampen [11], and write the normalized concentration relative to the interacting species as

$$\frac{n_i}{N} = \phi_i(t) + \frac{\xi_i}{\sqrt{N}}, \quad \frac{m_i}{N} = \psi_i(t) + \frac{\eta_i}{\sqrt{N}}, \quad (5)$$

where ξ_i and η_i stand for the stochastic contribution. The ansatz (5) is motivated by the central limit theorem and holds provided the dynamics evolve far from the absorbing boundaries (extinction condition). Here $1/\sqrt{N}$ plays the role of a small parameter and paves the way to a perturbative analysis of the master equation. At the leading order one recovers the mean-field equations, while the fluctuations are characterized as next to leading corrections. The following section is devoted to discussing the system dynamics, according to its mean-field approximation.

III. MEAN-FIELD APPROXIMATION AND THE TURING INSTABILITY

Performing the perturbative calculation one ends up with the following system of partial differential equations for the $\phi_i(t)$ and $\psi_i(t)$ in cell i:

$$\partial_\tau\phi_i = -b\phi_i - d\phi_i + a(1-\phi_i-\psi_i) + c\phi_i^2\psi_i + \mu[\Delta\phi_i + \phi_i\Delta\psi_i - \psi_i\Delta\phi_i],$$

$$\partial_\tau\psi_i = b\phi_i - c\phi_i^2\psi_i + \delta[\Delta\psi_i + \psi_i\Delta\phi_i - \phi_i\Delta\psi_i], \quad (6)$$

where $\tau = t/(N\Omega)$. In Eq. (6) we have introduced the discrete Laplacian operator Δ acting on a generic function f_i as

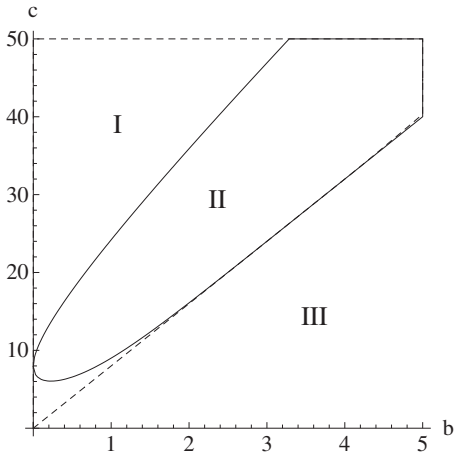

FIG. 1. The nature of the fixed point $(\hat{\phi}_3,\hat{\psi}_3)$ as a function of the parameters (b,c): in region I the fixed point is a stable node, while in II it is a stable spiral. The dashed line $c=8b$ delineates region III where the fixed point disappears, following a saddle-node bifurcation.

$$\Delta f_i = \frac{2}{z}\sum_{j\in i}(f_j - f_i). \quad (7)$$

The above sum runs on the first neighbors, which we assume to total in z. The limit $\Omega\to\infty$ corresponds to shrinking the lattice spacing l to zero and so obtaining the continuum mean-field description. In this limit the system (6) converges to

$$\partial_\tau\phi = -b\phi - d\phi + a(1-\phi-\psi) + c\phi^2\psi_i + \mu[\nabla^2\phi + \phi\nabla^2\psi - \psi\nabla^2\phi],$$

$$\partial_\tau\psi = b\phi - c\phi^2\psi + \delta[\nabla^2\psi + \psi\nabla^2\phi - \phi\nabla^2\psi], \quad (8)$$

where the population fractions go over the population densities and the rescaling $\mu\to\mu l^2$ and $\delta\to\delta l^2$ have been performed [14]. As also remarked in [5], cross-diffusive terms of the type $\phi\nabla^2\psi - \psi\nabla^2\phi$ appear in the mean-field equations, as a relic of the microscopic rules of interaction. More precisely, they arise as a direct consequence of the finite carrying capacity hypothesis. This observation materializes in a crucial difference with respect to the heuristically proposed reaction-diffusion schemes and points to the need for an extended Turing analysis, i.e., derive the generalized conditions yielding to organized spatial structures. Before addressing this specific issue, we start by discussing the homogeneous fixed point of Eq. (8). From hereon we will set $a=d=1$, a choice already made in [12] for the original Brusselator model and which will make possible to visualize our conclusion in the reference plan (b,c) for any fixed ratio of the diffusivity amount δ and μ.

A. Homogeneous fixed points

Plugging $a=d=1$ into Eqs. (8) and looking for homogeneous solutions implies

$$\begin{cases} \dot{\phi} = (1-\phi-\psi) - (1+b)\phi + c\phi^2\psi, \\ \dot{\psi} = b\phi - c\phi^2\psi. \end{cases} \tag{9}$$

As an important remark we notice that in the diluted limit $\phi, \psi \ll 1$, the system tends to the mean-field of the original Brusselator model, as, e.g., reported in [12]. For a proper tuning of the chemical parameters (assigning significantly different strength) one can prove that, if initialized so to verify the diluted limit, the system stays diluted all along its subsequent evolution. As a corollary, the diluted solution is contained in the formulation of the Brusselator here considered, this latter being therefore regarded as a sound generalization of the former. Notice that when operating under diluted conditions, the cross-diffusive terms appearing in the spatial equations (8) can be neglected and the standard reaction-diffusion scheme recovered. Again, let us emphasize that it is the finite carrying capacity assumption that modifies the mean-field description.

System (9) admits three fixed points, namely,

$$\begin{cases} \hat{\phi}_1 = 0, \\ \hat{\psi}_1 = 1, \end{cases} \quad \begin{cases} \hat{\phi}_2 = \dfrac{c - \sqrt{-8bc + c^2}}{4c}, \\ \hat{\psi}_2 = \dfrac{1}{2} + \dfrac{\sqrt{-8bc + c^2}}{2c}, \end{cases} \quad \begin{cases} \hat{\phi}_3 = \dfrac{c + \sqrt{-8bc + c^2}}{4c}, \\ \hat{\psi}_3 = \dfrac{1}{2} - \dfrac{\sqrt{-8bc + c^2}}{2c}. \end{cases} \tag{10}$$

The first of the above corresponds to the extinction of the species X: it exists for any choice of the freely changing parameters b, c and corresponds to a stable attractor for the dynamics. This solution is not present in the original Brusselator mean-field equations and its origin can be traced back to the role played by the limited capacity of the container.

The remaining two fixed points are, respectively, a saddle point and a (nontrivial) stable attractor. They both manifest when the condition $-8b+c>0$ is fulfilled. The saddle point partitions the available phase space into two domains, each defining the basin of attraction of the stable points. When $c=8b$ a saddle-node bifurcation occurs: the fixed points $(\hat{\phi}_2, \hat{\psi}_2)$ and $(\hat{\phi}_3, \hat{\psi}_3)$ collide to eventually disappear. The finite carrying capacity that follows the "urn representation" of the Brusselator dynamics destroys the limit cycle solution, which is instead found in its celebrated classical analogue [12]: no periodic solutions are found in the mean-field approximation, unless the diluted limit is considered. The specific nature of fixed point $(\hat{\phi}_3, \hat{\psi}_3)$ changes as a function of the parameters (b, c), as illustrated in Fig. 1. In region I, it is a stable node, while in II it is a stable spiral. Region III identifies the parameters values for which it disappears. We are here concerned with the stability of the homogeneous fixed point $(\hat{\phi}_3, \hat{\psi}_3)$ to inhomogeneous perturbation: can an instability develop and yield to organized Turing-like spatial patterns?

B. Extending the Turing instability mechanism: The effect of cross-diffusion

To answer the previous question one has to perform a linear stability analysis around the selected homogeneous solution $(\hat{\phi}_3, \hat{\psi}_3)$, hereafter termed $(\hat{\phi}, \hat{\psi})$, accounting for the effect of nonhomogeneous perturbation. The formal development is closely inspired by the original Turing calculation, but now the effects of cross-diffusive terms need to be accommodated for. The technical details of the derivation are enclosed in the annexed Appendix, where the most general problem is defined and inspected. We will here take advantage from the conclusion therein reached and present the results relative to the Brusselator model. In this specific case $a=d=1$, the dispersion relation (A7) reads in particular

$$\lambda(k^2) = \mathcal{A} + k^2\mathcal{B} + \frac{1}{16c}[\mathcal{C} + \mathcal{D}k^2 + \mathcal{E}k^4]^{1/2}, \tag{11}$$

where

$$\mathcal{A} = -1 + \frac{3b}{4} - \frac{c}{16} - \frac{1}{16}\sqrt{c(-8b+c)},$$

$$\mathcal{B} = -\frac{3\delta}{8} + \frac{\sqrt{c(-8b+c)}\,\delta}{8c} - \frac{\mu}{4} - \frac{\sqrt{c(-8b+c)}\,\mu}{4c},$$

$$\mathcal{C} = 256c^2 + 128bc^2 + 144b^2c^2 - 32c^3 - 32bc^3 + 2c^4 + \sqrt{c(-8b+c)}(-32c^2 - 24bc^2 + 2c^3),$$

$$\mathcal{D} = -64c^2\delta + 16bc^2\delta + 8c^3\delta + 128c^2\mu + 96bc^2\mu - 16c^3\mu + \sqrt{c(-8b+c)}\cdot(-64c\delta - 80bc\delta + 8c^2\delta + 128c\mu + 32bc\mu - 16c^2\mu),$$

$$\mathcal{E} = -32bc\delta^2 + 40c^2\delta^2 + 128bc\delta\mu - 32c^2\delta\mu - 128bc\mu^2 + 32c^2\mu^2 + \sqrt{c(-8b+c)}(-24c\delta^2 - 32c\delta\mu + 32c\mu^2). \tag{12}$$

The perturbation gets amplified if $\lambda(k^2)>0$ over a finite interval of k values. The edges, k_1 and k_2, of the interval are identified by imposing $\lambda(k^2)=0$, which returns the following results:

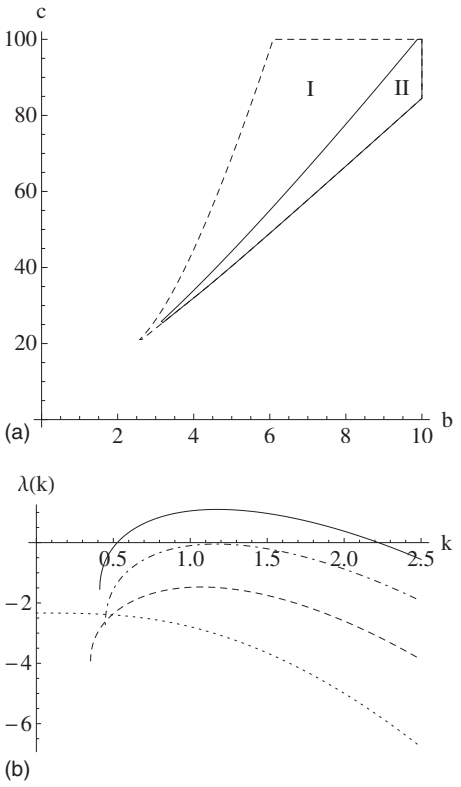

FIG. 2. Upper panel: the domain corresponding to the Turing instability are displayed in the (b,c) plan for $\delta=15$ and $\mu=1$. The solid line (zone 2) delineates the region calculated when accounting for the cross-diffusive contribution, the dashed one (zone 1) stands for the conventional Turing analysis where diffusion is modeled via Laplacian operators (i.e., disregarding cross-diffusion). Lower panel: dispersion relation $\lambda(k)$ vs k. Here $c=70$ and $b=3,5,6,7$ (starting from the dotted bottom curve).

$$k_{1,2}=\frac{1}{2\sqrt{2b\delta\mu}}[2c\delta(b-1)+8b^2(\mu-\delta)-bc\mu+\sqrt{c(-8b+c)}\times(2\delta-2b\delta-b\mu)\pm(\mathcal{F}+\sqrt{c(-8b+c)}\mathcal{G})^{1/2}]^{1/2}, \quad (13)$$

where

$$\mathcal{F}=2\{4c^2\delta^2-8bc(2+c)\delta^2+32b^4(\delta-\mu)^2-4b^3c(8\delta^2-2\delta\mu+3\mu^2)+b^2c[4(12+c)\delta^2+c\mu^2]\},$$

$$\mathcal{G}=2\{-4c\delta^2+8bc\delta^2+8b^3(2\delta^2-\delta\mu-\mu^2)+b^2[-4(4+c)\delta^2-16\delta\mu+c\mu^2]\}. \quad (14)$$

By making use of conditions Eq. (A9) as derived in the Appendix, the predicted region for the Turing instability is traced in the (b,c) parameter space for an assigned ratio of mutual diffusivity, see Fig. 2. When compared to the conventional Turing analysis, based on the heuristically hypothesized reaction-diffusion scheme [i.e., removing the cross terms in Eq. (8)], the region of inhomogeneous instability shrinks, the condition for spatial self-organization becoming even more peculiar than so far believed.

Up to now we have carried out the analysis in the continuous mean-field scenario neglecting the role of finite size corrections. Stochastic fluctuations can however amplify due to an inherent resonant mechanism and consequently give rise to a large scale spatial order, similar to that predicted within the Turing interpretative picture [6]. The following section is entirely devoted to clarifying this important point.

IV. ROLE OF STOCHASTIC NOISE AND THE POWER SPECTRUM OF FLUCTUATIONS

At the next to leading order in the van Kampen perturbative development one ends up with a Fokker-Planck equation for the probability distribution of the fluctuations $\Pi(\boldsymbol{\xi},\boldsymbol{\eta},t)=P(\mathbf{n},\mathbf{m},t)$ where the vectors $\boldsymbol{\xi}$ and $\boldsymbol{\eta}$ have dimensions Ω and respective components ξ_i and η_i. The derivation is lengthy but straightforward and the reader can refer to, e.g., [5,7]. for a detailed account on the mathematical technicalities. We will here report on the outcome of the calculation in terms of the predicted power spectra of the fluctuations close to equilibrium. In complete analogy with, e.g., Eqs. (36) and (37) of [5] the latter can be written as

$$P_{k,X}(\omega)=\langle|\boldsymbol{\xi}_k(\omega)|^2\rangle,$$

$$P_{k,Y}(\omega)=\langle|\boldsymbol{\eta}_k(\omega)|^2\rangle,$$

where the ω and k stand, respectively, for Fourier temporal and spatial frequencies [15]. Exploiting the formal analogy between the governing Fokker-Planck equation and the equivalent Langevin equation one eventually obtains (see Eqs. (38) and (39) in [5])

$$P_{k,X}(\omega)=\frac{\mathbf{C}_1+\mathbf{B}_{k,11}\omega^2}{(\omega^2-\Omega_{k,0}^2)^2+\Gamma_k^2\omega^2},$$

$$P_{k,Y}(\omega)=\frac{\mathbf{C}_2+\mathbf{B}_{k,22}\omega^2}{(\omega^2-\Omega_{k,0}^2)^2+\Gamma_k^2\omega^2},$$

where

$$C_{k,X}(\omega)=\mathbf{B}_{k,11}M_{k,22}^2-2\mathbf{B}_{k,12}M_{k,12}M_{k,22}+\mathbf{B}_{k,22}M_{k,12}^2, \quad (15)$$

$$C_{k,Y}(\omega)=\mathbf{B}_{k,22}M_{k,11}^2-2\mathbf{B}_{k,12}M_{k,21}M_{k,11}+\mathbf{B}_{k,11}M_{k,21}^2. \quad (16)$$

The 2×2 matrix M_k of elements $M_{k,ij}$ reads

$$\mathbf{M}_k=\begin{pmatrix}-2-b+2c\hat{\phi}\hat{\psi}+\mu(1-\hat{\psi})\Delta_k & -1+c\hat{\phi}^2+\mu\hat{\phi}\Delta_k\\ b-2c\hat{\phi}\hat{\psi}+\delta\hat{\psi}\Delta_k & -c\hat{\phi}^2+\delta(1-\hat{\phi})\Delta_k\end{pmatrix}, \quad (17)$$

and the elements $\mathbf{B}_{k,ij}$, respectively, are

$$\mathbf{B}_{k,11}=1+b\hat{\phi}-\hat{\psi}+c\hat{\phi}^2\hat{\psi}-2\mu\hat{\phi}\Delta_k+2\mu\hat{\phi}^2\Delta_k+2\mu\hat{\phi}\hat{\psi}\Delta_k, \quad (18)$$

$$\mathbf{B}_{k,12}=-b\hat{\phi}-c\hat{\phi}^2\hat{\psi}, \quad (19)$$

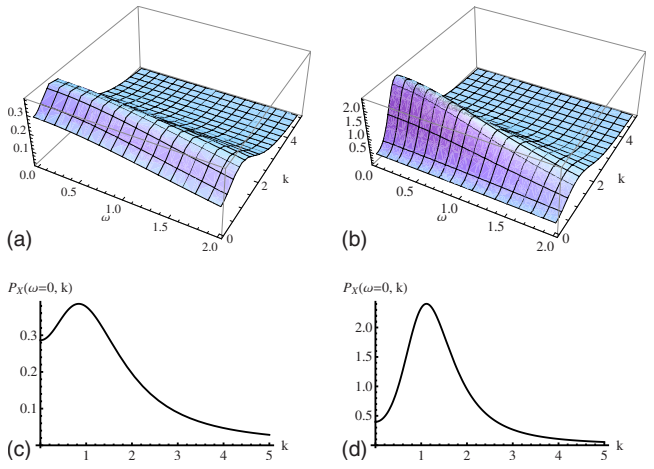

FIG. 3. (Color online) Upper panels: the power spectra $P_{k,X}(\omega)$ for $c=70$ and $b=3,6$ (going from left to right). Here $\delta=15$ and $\mu=1$. The selected values of b and c fall outside the region of Turing instability, as follows the mean-field linear stability calculation (see Fig. 2). Lower panels: the power spectra $P_{k,X}(0)$ plotted vs k so to enable one to appreciating the range of excited spatial wavelengths. This latter approximately matches that found in the realm of the Turing mean-field calculation (see Fig. 2), implying similar characteristic of the spatially ordered structures.

$$\mathbf{B}_{k,22} = b\hat{\phi} + c\hat{\phi}^2\hat{\psi} - 2\delta\hat{\psi}\Delta_k + 2\delta\hat{\phi}\hat{\psi}\Delta_k + 2\delta\hat{\psi}^2\Delta_k, \quad (20)$$

with the additional condition $\mathbf{B}_{k,12}=\mathbf{B}_{k,21}$. Finally, $\Omega_{k,0}^2 = \det \mathbf{M}_k$, $\Gamma_k = -\mathrm{tr}\,\mathbf{M}_k$, and the Fourier transform of the Laplacian $\Delta_k = 2[\cos(kl)-1]$. In the continuum limit, the cell size goes to zero and Δ_k scales as $\Delta_k \sim k^2$ [5].

We are now in a position to represent the power spectrum of the fluctuations as predicted by the system size expansion. In Fig. 3 we display a selection of power spectra relative to one population and for different values of the parameter b, at fixed c and diffusivity amount (see caption). The snapshots refer to a region of the parameter space for which we do not expect spatial order to appear, based on the Turing paradigm. However, and beyond the simplified mean-field viewpoint, a clear spatial peak is displayed, which gains in potency as the boundary of the Turing domain is being approached. Physically, it seems plausible to assume that the demographic noise can modify the dispersion relation. As a consequence, the curve $\lambda(k)$, negative defined beyond the region of Turing instability, can locally cross the zero line, taking positive values in correspondence of specific k. These latter modes get therefore destabilized, yielding to quasi-Turing structures. Clearly, the k candidate to drive the stochastic instabilities are the ones close to $k_{\max}$, the wave number that identifies the position of the maximum of the dispersion relation. If the above scenario is correct, $k_{\max}$ should then be reasonably similar to the k value that locates the peak position in the power spectra $P(k,\cdot)(0)$. In Fig. 4 such comparison is drawn, for both species and over a window of b values, confirming the adequacy of the proposed interpretation. Based on the above, we can convincingly argue that the spatial modes here predicted represent an ideal continuation of the Turing structures beyond the region of parameters de-

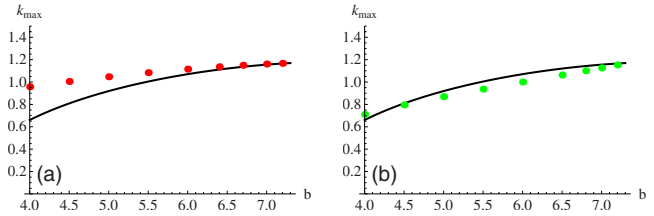

FIG. 4. (Color online) Left panel: symbols refer to the values in k that identify the maximum of the function $P_{k,X}(0)$, here plotted as a function of b. The solid line stands for the position of the maximum of the mean-field dispersion relation $\lambda(k)$. Parameters are set as in Fig. 3. Right panel: as in the left panel, but now the symbols refer to species Y.

puted to the mean-field instability and, for this reason, we suggest to refer to them as to *stochastic Turing patterns*.

The fact that spatial order appears for a wider range of the control parameter is further confirmed by visual inspection of Fig. 5, where the region of stochastic induced spatial organization, delineated from the power spectra calculated above, is depicted and compared to the corresponding mean-field prediction. Notice that the domains yielding to stochastic Turing patterns structures are different depending on the considered species. This observation marks yet another difference with respect to the standard mean-field theory. We can in fact expect to observe spatially ordered structures for just one of the two species, while the other is homogenously distributed.

As an additional point, we consider the case $\delta=\mu=1$. This choice cannot yield to the genuine Turing order, a pronounced difference in the relative diffusivity rates being an unavoidable prerequisite. As opposed to the classical picture, stochastic Turing patterns can still emerge as demonstrated in Fig. 6.

From the above expressions for the power spectra, one can also show that for $\mu=\delta=0$ (the aspatial limit) quasiperiodic time oscillations manifest in the concentrations. This is an effect of inner stochastic noise, which restores the oscil-

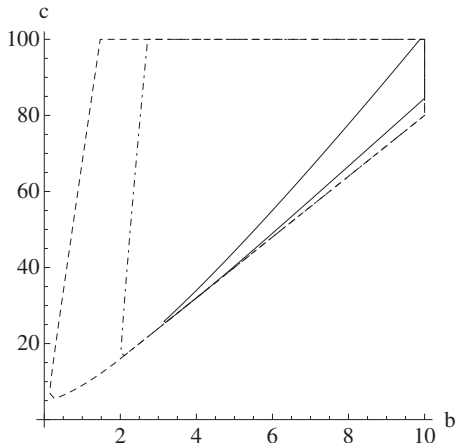

FIG. 5. The extended domain of Turing-like instability predicted by the stochastic based analysis: the dashed line refers to species X, while the dot-dashed to species Y. The stochastic Turing region is confronted to the corresponding mean-field solution (solid line, also depicted in Fig. 3).

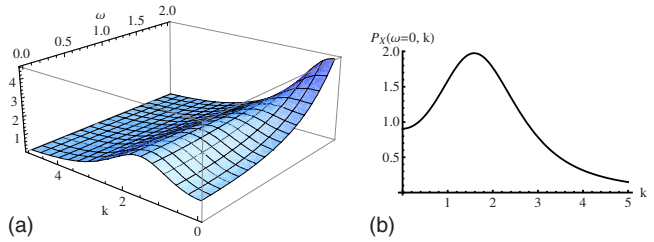

FIG. 6. (Color online) Left panel: the power spectra $P_{k,X}(\omega)$ for $a=d=1$, $c=70$, and $b=8$. Spatial and temporal peaks appear now to be decoupled. Right panel: the corresponding power spectra $P_{k,X}(0)$ plotted vs k. A clear peak is displayed.

lations destroyed by the introduction of the carrying capacity. In general terms, self-oscillatory dynamics could be possibly understood, as resulting from the discrete nature of the medium, a scenario alternative to any *ad hoc* mean-field interpretation.

V. CONCLUSION

Spatially organized patterns are reported to occur in a large gallery of widespread applications and are currently interpreted by resorting to the paradigmatic Turing picture. This vision, though successful, relies on a mean-field description of the relevant reaction-diffusion schemes, often guessed on purely heuristic basis. An alternative scenario would require accounting for the intimate microscopic dynamics and so encapsulating the effect of the small scale graininess. This latter translates into stochastic fluctuations that, under specific conditions, can amplify and so give rise to organized spatio-temporal patterns. In this paper we have considered a microscopic model of Brusselator, and shown that Turing-like patterns can indeed emerge beyond the parameter region predicted by the conventional Turing theory and due to the role of finite size corrections to the mean-field idealized dynamics. This result is obtained via a system size expansion, which enables us to return closed analytical expressions for the power spectra of fluctuations. Our results agree with the conclusion reached in [6] for another model and employing different analytical tools. Organized patterns can therefore occur more easily than expected, an observation that can potentially help reconciling theory and observations. In particular we find stochastic Turing patterns to emerge for $\delta \sim \mu$, a condition for which Turing order is prevented to occur.

ACKNOWLEDGMENTS

D.F. wishes to thank Alan J. McKane for interesting discussions and for pointing out reference [6]. F.D.P. wishes to thank Javier Buceta for stimulating discussion. F.D.P thanks financial support from the ESF Short Visit Grant within the framework of the ESF activity entitled "Functional Dynamics in Complex Chemical and Biological Systems."

APPENDIX

Let us start by the generic set of partial differential equations

$$\partial_t \phi = f(\phi,\psi) + \mu[\nabla^2\phi + \phi\nabla^2\psi - \psi\nabla^2\phi],$$

$$\partial_t \psi = g(\phi,\psi) + \delta[\nabla^2\psi + \psi\nabla^2\phi - \phi\nabla^2\psi], \tag{A1}$$

which explicitly allow for cross-diffusive contributions. We choose to deal with zero flux boundary conditions.

Assume that in absence of diffusion (homogeneous setting) the model tends towards a fixed point specified by $(\hat{\phi},\hat{\psi})$. In other words, $\hat{\phi},\hat{\psi}$, do not depend over space variables. Allowing for diffusion, and imposing $\mu \neq \delta$, can make the system unstable to spatial perturbation. To clarify this point, let us start by considering the Jacobian matrix for $\mu = \delta = 0$

$$\mathbf{J} = \begin{pmatrix} f_\phi & f_\psi \\ g_\phi & g_\psi \end{pmatrix}. \tag{A2}$$

The fixed point $(\hat{\phi},\hat{\psi})$ is linearly stable if $\mathbf{J}$ has positive determinant and negative trace

$$\det \mathbf{J} = f_\phi g_\psi - g_\phi f_\psi > 0, \quad \mathrm{tr}\, \mathbf{J} = f_\phi + g_\psi < 0. \tag{A3}$$

Assuming Eq. (A3) to hold one can proceed with a linearization of Eq. (A1) (with $\mu,\delta \neq 0$) around $(\hat{\phi},\hat{\psi})$ and so looking for the sought condition of instability. Define $\mathbf{x} = \begin{pmatrix} \phi-\hat{\phi} \\ \psi-\hat{\psi} \end{pmatrix}$, then Eq. (A1) becomes

$$\partial_t \mathbf{x} = \mathbf{J}\mathbf{x} + \mathbf{D}\nabla^2\mathbf{x}, \quad \mathbf{D} = \begin{pmatrix} \mu(1-\hat{\psi}) & \mu\hat{\phi} \\ \delta\hat{\psi} & \delta(1-\hat{\phi}) \end{pmatrix}. \tag{A4}$$

Define the eigenfunctions of the Laplacian operator as

$$(\nabla^2 + k^2)\mathbf{W}_k(\mathbf{r}) = 0, \quad \mathbf{r} \in H,$$

and write the solution to Eq. (A4) in the form

$$\mathbf{x}(t,\mathbf{r}) = \sum_k e^{\lambda t} a_k \mathbf{W}_k(\mathbf{r}). \tag{A5}$$

Assume $\mu = 1$, or equivalently label with δ the ratio of the two diffusivities (after proper rescaling of the rate coefficients). Substituting ansatz (A5) into Eq. (A4) yields

$$e^{\lambda t}[\mathbf{J} - k^2\mathbf{D} - \lambda\mathbf{1}]\mathbf{W}_k = 0,$$

which implies that the system admits a solution iff the matrix $\mathbf{J} - k^2\mathbf{D} - \lambda\mathbf{1}$ is singular, i.e.,

$$\det(\mathbf{J} - k^2\mathbf{D} - \lambda\mathbf{1}) = 0. \tag{A6}$$

Label the solutions of Eq. (A6) as $\lambda_1(k^2)$ and $\lambda_2(k^2)$: they can be interpreted as dispersion relation, specifying the time scale of departure (or convergence) of the k-th mode towards the deputed fixed point. If at least one of the two solutions displays a positive real part, the mode is unstable, and drives the system dynamics towards a nonhomogeneous configuration in response to the initial perturbation. Manipulating the determinant, Eq. (A6) takes the form

$$\lambda^2 + \lambda q(k^2) + h(k^2) = 0, \tag{A7}$$

where

$$q(k^2) = k^2 + k^2\delta(1 - \hat{\phi} - \hat{\psi}) - f_\phi - g_\psi,$$

$$h(k^2) = k^4\delta - k^4\hat{\phi}\delta - k^4\hat{\psi}\delta - k^2\delta f_\phi + k^2\hat{\phi}\delta f_\phi + k^2\hat{\psi}\delta f_\psi + k^2\hat{\phi}g_\phi - f_\psi g_\phi - k^2 g_\psi + k^2\hat{\psi}g_\psi + f_\phi g_\psi.$$

$\lambda_1(k^2)$ and $\lambda_2(k^2)$ are obtained as roots of Eq. (A7). The actual dispersion relation, $\lambda(k^2)$ in the main body of the paper, is the one that displays the largest real part. We notice that (i) $q(k^2)$ is always positive as $\delta > 0$ by definition; (ii) $(1-\hat{\phi}-\hat{\psi}) > 0$ as $\hat{\phi}$ and $\hat{\psi}$ are concentrations; (iii) $-f_\phi - g_\psi > 0$ due to Eq. (A3). Left-hand side of Eq. (A7) is hence a parabola with the concavity pointing upward and the minimum positioned in the half-plane of negative abscissa. In conclusion a necessary and sufficient condition for the existence of real roots is $h < 0$ where

$$h(k^2) = \tilde{a}k^4 + \tilde{b}k^2 + \tilde{c}, \quad \begin{cases} \tilde{a} = \delta(1 - \hat{\phi} - \hat{\psi}), \\ \tilde{b} = -\delta f_\phi - g_\psi + \hat{\phi}(\delta f_\phi + g_\phi) + \hat{\psi}(\delta f_\psi + g_\psi), \\ \tilde{c} = \det \mathbf{J}, \end{cases} \tag{A8}$$

with $\tilde{a} > 0, \tilde{c} > 0$. The condition for $h < 0$ corresponds to $\tilde{b} < 0$ and $\tilde{b}^2 - 4\tilde{a}\tilde{c} > 0$. Summing up the condition for the generalized Turing instability reads

$$(\delta f_\phi + g_\psi) - \hat{\phi}(\delta f_\phi + g_\phi) - \hat{\psi}(\delta f_\psi + g_\psi) > 0,$$

$$[(\delta f_\phi + g_\psi) - \hat{\phi}(\delta f_\phi + g_\phi) - \hat{\psi}(\delta f_\psi + g_\psi)]^2 > 4\delta(1 - \hat{\phi} - \hat{\psi})\det \mathbf{J}, \tag{A9}$$

together with Eq. (A3).

[1] A. M. Turing, Philos. Trans. R. Soc. London, Ser. B **237**, 37 (1952).
[2] J. Buceta and K. Lindenberg, Phys. Rev. E **66**, 046202 (2002).
[3] J. D. Murray, *Mathematical Biology*, 3rd ed. (Springer, New York, 2003).
[4] A. J. McKane and T. J. Newman, Phys. Rev. Lett. **94**, 218102 (2005).
[5] C. A. Lugo and A. J. McKane, Phys. Rev. E **78**, 051911 (2008).
[6] T. Butler and N. Goldenfeld, Phys. Rev. E **80**, 030902(R) (2009).
[7] P. de Anna, F. Di Patti, D. Fanelli, A. McKane, and T. Dauxois, e-print arXiv:1001.4908.
[8] P. Glandsdorff and I. Prigogine, *Thermodynamics Theory of Structure Stability and Fluctuations* (Wiley, New York, 1971).
[9] B. P. Belousov, *Collection of Short Papers on Radiation Medicine for 1958* (Med. Publ., Moschow, 1959); A. M. Zhabotinsky, Biofizika **9**, 306 (1964).
[10] S. Strogatz, *Non Linear Dynamics and Chaos: With Applications to Physics, Biology, Chemistry and Engineering* (Perseus Book Group, Cambridge, MA, 2001).
[11] N. G. van Kampen, *Stochastic Processes in Physics and Chemistry*, 3rd ed. (Elsevier, Amsterdam, 2007).
[12] R. P. Boland, T. Galla, and A. J. McKane, Phys. Rev. E **79**, 051131 (2009).
[13] Working with the empties E implies imposing a finite carrying capacity in each microcell. This procedure defines the so called "urn protocol," and allows for a technically easier implementation of the van Kampen expansion as presented in Ref. [4]. On the other hand, and besides technical reasons, assuming a limited capacity in space is a reasonable physical request. It is therefore interesting to explore how such a choice reflects on the subsequent analysis. Let us anticipate that the presence of the empties E will sensibly modify the mean-field phase diagram of the Brusselator model, as concerns both the homogeneous and the spatial dynamics. Conversely, the observation that the Turing region gets enlarged by demographic noise holds true, irrespectively of the specific urn representation here invoked (Ref. [6]).
[14] The original parameters μ and δ quantify the ability of the molecules to exit/enter a given patch of size l. When l gets reduced, μ (resp. δ) should correspondingly increase, so that the quantity μl^2 (resp. δl^2) converges to a finite value (the physical diffusivity) when the limit $\Omega \to \infty$ is taken. This latter value is in turn the one that enters the continuous equations (8).
[15] We define the Fourier transform f_k of a function $f_{\mathbf{j}}$ defined on a one dimensional lattice with spacing l as $f_k = l\Sigma_j \exp(-ik \cdot lj) f_{\mathbf{j}}$, see Ref. [5].